ELSEVIER

Polymer 44 (2003) 2773–2780

polymer

www.elsevier.com/locate/polymer

Radiation induced embrittlement of PTFE

B. Fayolle*, L. Audouin, J. Verdu

ENSAM 151 Bd de l'Hôpital, 75013 Paris, France

Received 12 September 2002; received in revised form 14 January 2003; accepted 28 January 2003

Abstract

The radiochemical degradation of polytetrafluoroethylene (PTFE) samples has been studied in air at dose rate 100 Gy/h for doses up to 5000 Gy, at ambient temperature. The polymer degradation has been monitored by DSC, tensile testing and Essential Work of Fracture (EWF) testing. Some fractured samples have been observed by scanning electron microscopy. The polymer undergoes a fast chain scission, its number average molar mass is divided by about 20 for a dose of 1000 Gy and tends towards a pseudo asymptotic value of ~ 20 kg mol^{-1} (against 6200 kg mol^{-1} initial value). The modulus and yield characteristics seem to be almost unaffected whereas ultimate properties undergo strong variations. The ultimate elongation ε_R and the EWF plastic work characteristic βw_p first increase and then decrease. The ultimate stress decreases and tends towards a pseudo asymptotic value. The mechanisms of radiation induced ultimate property changes are discussed. The first stage could be due to the destruction of non-extended tie molecules (due to the presence of very long chains) responsible for interfibrillar bridging during fracture. The (more classical) second stage is a progressive embrittlement due to the destruction of the entanglement network. The critical molar mass M_c' for embrittlement is such as $M_c' \sim 50M_e$, M_e being the molar mass between entanglements in the melt. This relationship could be a general characteristic of high crystallinity non-polar polymers.

Keywords: Polytetrafluoroethylene; Molar mass; Essential work of fracture

1. Introduction

Although Polytetrafluoroethylene (PTFE) exhibits very useful properties, in particular high chemical and thermal stability or a low coefficient of friction, its use under irradiation is limited. As a matter of fact, PTFE is highly sensitive to radiation: a very little modification induced by irradiation leads to embrittle the polymer. The cause of this process is often attributed to a mechanism of chain scission which reduces dramatically molar mass [1,2].

The aim of this article is to try to establish a quantitative relationship between the molar mass decrease and the embrittlement process in order to have a pertinent endlife criterion for lifetime prediction. There is, to our knowledge, no published work about this aspect on PTFE.

In the case of amorphous polymers, in contrast, the importance of the entanglement network in plastic deformation (in particular in crazing) is well recognized and the existence of a critical molar mass M_c' such as $M > M_c'$ the polymer is tough and eventually ductile whereas for $M < M_c'$ it is brittle, is sharply linked to the entanglement threshold so that:

$$M_C' = qM_e \tag{1}$$

where M_e is the molar mass between entanglements and q a factor ranging typically between 2 and 10 [3–5]. In the case of semi-crystalline polymers, plasticity mechanisms are different although the amorphous phase plays also a key role. Do the above scaling law remain valid in the case of PTFE? It will be tried, in the following, to answer this question.

To evaluate the fracture toughness of PTFE, strain at break or stress at break in tensile mode are the most commonly used properties [6]. This basic determination leads to very scattered results due to, for instance, eventual defects on the sample edge. To avoid these effects, a fracture mechanics approach appears to be more appropriated to characterize fracture. However, the linear elastic fracture mechanics fail to describe the fracture behaviour of highly ductile materials such as PTFE because it doesn't take into account the energy dissipated by ligament yielding. In such cases, the Essential Work of Fracture (EWF) method appears to be the most appropriate approach to characterize

* Corresponding author. Tel.: +33-1-4424-6413; fax: +33-1-4424-6382.
E-mail address: bruno.fayolle@paris.ensam.fr (B. Fayolle).

0032-3861/03/$ - see front matter © 2003 Elsevier Science Ltd. All rights reserved.
doi:10.1016/S0032-3861(03)00116-2

ductile fracture under plane stress conditions. The aim of this work is to study the beginning of the embrittlement process especially for low doses using classical tensile test and the EWF method to bring some new elements about the embrittlement process of PTFE.

In the EWF approach, the total work of rupture (W_f) is divided into two components: the essential work of fracture (W_e) and the non-essential work of fracture (W_p):

$$W_f = W_e + W_p \tag{2}$$

Schematically, the essential work of fracture is the work dissipated in the process zone and the non-essential work of fracture is the work dissipated in the outer plastic zone. The situation is sketched in Fig. 1(a). To obtain both components, the total work of fracture W_f, recorded during the mechanical test and comprising all the energy dissipated during the test, is expressed as:

$$W_f = \int P\mathrm{d}U = w_e l t + \beta w_p l^2 t \tag{3}$$

where P is the load, U the displacement, t the sample thickness and l the ligament length. So, per cross section unit, the specific total work of fracture (w_f) is expressed as:

$$w_f = W_f/lt = w_e + \beta w_p l \tag{4}$$

the component accounting for the essential work of fracture, w_e, and the plastic deformation term βw_p are expected to be independent of specimen geometry for a given sheet thickness, β being the shape factor of the plastic zone (Fig. 1(b)). It is assumed that β does not vary with the ligament length. A first approach considers that the fundamental parameter is w_e [7,8]. It seems, however, that a consensus exists on the fact that βw_p is linked to the plasticity development and so the ability of material to dissipate energy during the fracture process [9].

2. Experimental

2.1. Materials and exposure

The experiments were conducted with 1 mm tick plate of an industrial PTFE. Initial physico-chemical characteristics are given in Table 1.

Irradiations were realized in air with a relatively low dose rate: 100 Gy h^{-1}. Samples have been irradiated by Co^{60} gamma rays at room temperature. The set of absorbed dose is shown in Table 1. For the EWF experiments, only absorbed doses below 1500 Gy have been studied because for higher doses, PTFE displays a brittle behaviour incompatible with EWF test protocol [10].

2.2. Physical characterization

Thermal analysis was carried out using a Netzsch 200 differential scanning calorimeter (DSC). Heat of fusion and crystallisation were determined from their peak areas. The reported data correspond to the average of ten experiments at 10 °C min^{-1} heating rate.

Molar masses were determined from heat of crystallisation according to Suwa's method. This method is based on an empirical relationship [11]:

$$M_n = 2.1 \times 10^{10} \Delta H_C^{-5.16} \tag{5}$$

where M_n is the number average molar mass in g mol^{-1} and ΔH_C is the heat of crystallization in cal/g. It is noteworthy that this relationship induces necessarily very scattered values of M_n because of high exponent value and incertitude on experimental determination of ΔH_C.

The X-ray diffraction patterns were recorded with a conventional Bragg–Brentano diffractometer equipped with a solid germanium detector. Diffraction diagram of PTFE sample were performed with a scanning speed of 1.5° min^{-1}. The wavelength was Fe K_α ($\lambda = 1.9374$ Å).

Fracture surfaces were observed using a JEOL scanning electron microscope at 5 kV on gold-coated samples.

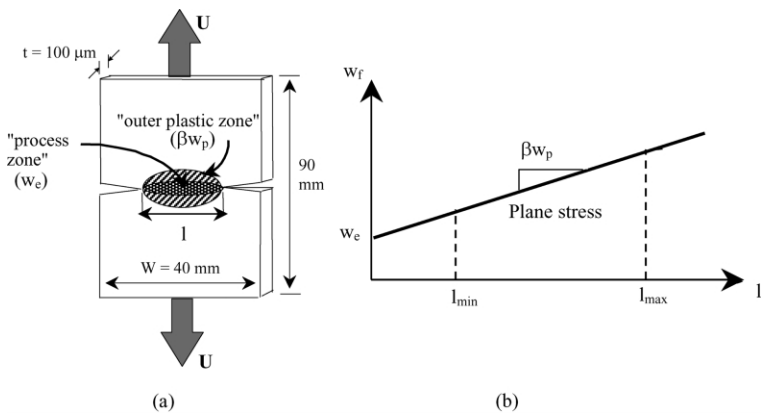

Fig. 1. Theoretical assignment and graphical determination of w_e and βw_p parameters from a w_f vs l plot.

Table 1
Changes in thermal properties of initial and irradiated PTFE.

Irradition dose (Gy)	$T_{\alpha C}$ (°C)	T_f (°C)	H_f (J/g)	T_C (°C)	H_C (J/g)	M_n (kg mol^{-1})
0	24	333	23	312	21	6 200
250	24.5	334	36.4	312	30	1 640
500	23.9	335	39.8	310	36	330
1000	23.7	335	37.1	311	36.2	320
1500	24.1	335	49.3	310	43.8	120
2000	24.3	335	48.6	310	47.7	90
3000	24	336	53.6	309	56.6	30
4000	24.7	336	50.5	309	55.5	30
5000	23.5	335.9	53.6	310	61	20

2.3. Mechanical test

The mechanical tests were carried out on a tensile testing machine INSTRON 4502. All mechanical tests were performed at a constant crosshead displacement rate at 5 mm min^{-1}.

For tensile measurements, dumbbell shaped specimens with a calibrated length of 20 mm and a width of 4 mm were cut from the plate with a MTS H4 stamp. Only ultimate engineering strains are reported here; no corrections were made for thickness and width changes induced by necking.

For EWF testing, rectangular coupons of width (W) 40 mm and overall length 90 mm long were cut in PTFE plate. Test samples with Double Edges Notch Tensile (DENT) geometry were prepared by razor notching giving ligament lengths (l) ranging from 6 to 16 mm [10]. The ligament length is controlled after test with the help of an optical microscope coupled with a computer controlled X–Y table.

A load–displacement diagram was recorded to evaluate the total work of fracture, W_f, for each ligament length. The influence of the ligament length on the load-displacement curves is shown in Fig. 2. These curves display a maximum which corresponds to blunting due to complete ligament yielding. Beyond this maximum, a slow load decrease indicates slow stable crack propagation into the yielded ligament, perpendicularly to the load direction. The test is valid only if both plastic zones are inter-connected along the horizontal axis defined by the initial notches and thus perpendicular to the loading axis.

In the plane stress state under consideration, w_f is expected to vary linearly with l (Fig. 1(b)). For a given sample geometry, it is thus necessary to determine the range of ligament length within the linear relationship (Eq. 4) is valid.

The test protocol recommends the use of ligament lengths lower than $l_{max} < W/3$ [10]. This last condition has to preserve the homothetic character of the load–displacement curves as it is shown in Fig. 2. The lower limit for the ligament length corresponds usually to the transition from plane stress to plane strain [10]. The maximum net section stress σ_n in the ligament should not exceed the theoretical stress at the onset of yielding. Consequently, the minimum ligament length must correspond to the condition $\sigma_n < 1.15\sigma_y$ [10]. In order to satisfy this condition and to remain in the linear domain, the ligament length was varied between 6 and 16 mm. A set of 20 specimens with varying ligament length was tested to evaluate w_e and βw_p. Values of w_e and βw_p were calculated from the experimental w_f versus ligament length plots by linear regression.

3. Results

3.1. Structural modifications

Modifications induced by irradiation and monitored by DSC are reported in Table 1. No changes in terms of crystal disordering transition $T_{\alpha C}$ [12] or melting temperature T_f were observed. A slow increase of melting enthalpy H_f is detected (Fig. 3). One can assume, however, in a first approximation that crystalline phase appears to be not significantly affected by irradiation. Complementary wide-angle X-ray scattering determinations confirm this hypothesis. On the other hand, crystallisation parameters are largely modified by irradiation. Using Suwa's relationship, the number average molar mass M_n calculated from heat of crystallisation decreases from the beginning of the exposure: Irradiation consequences consist essentially on a chain scission process. In Fig. 4, the changes of molar mass

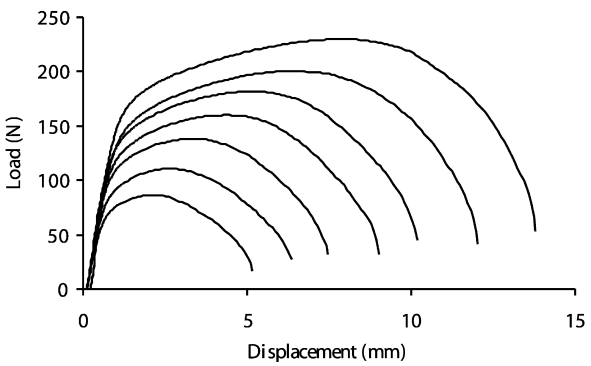

Fig. 2. Load–displacement curves for ligament lengths varying from 6 to 16 mm.

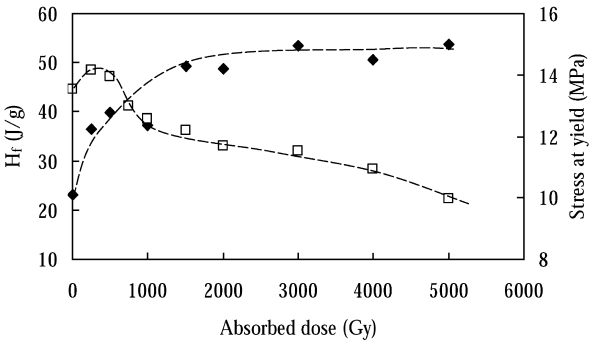

Fig. 3. Enthalpy of melting (◆) and yield stress (□) as a function of absorbed dose.

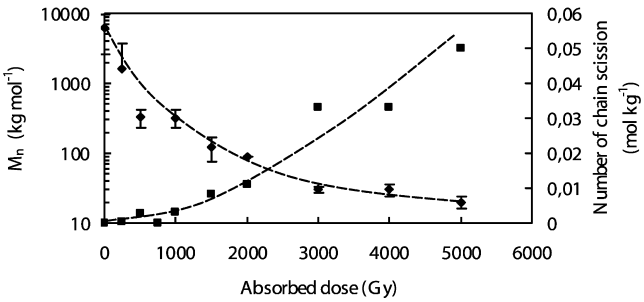

Fig. 4. Number average molar mass (◆) and number of chain scission (■) as a function of absorbed dose.

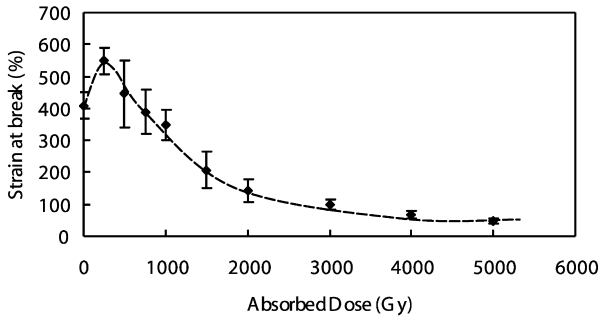

Fig. 6. Changes in strain at break vs absorbed dose.

in log scale as a function of absorbed dose are shown. From an initial value of 6000 kg mol^{-1}, M_n decreases to reach an asymptotic value close to 20 kg mol^{-1}.

3.2. Uniaxial tensile test

From tensile test measurements, changes of yield stress (σ_y) are also reported in Fig. 3. Let us recall that yield stress, in semi-crystalline polymers like PE, is essentially linked to the crystalline phase whereas ultimate properties are rather linked to amorphous phase [13]. As proposed above, the constant value (or a slight decrease from 14 to 12 MPa) of σ_y with irradiation confirms that the crystalline structure is practically not affected. Stress at break σ_R varies significantly from the beginning of exposure (Fig. 5). However, many authors consider better the strain at break (ε_R) because this latter is the most pertinent parameter to monitor embrittlement [14–16]. In Fig. 6, ε_R is plotted against absorbed dose. For the low doses (250 and 500 Gy), one can observe surprisingly an increase of ε_R whereas beyond 750 Gy, ε_R decreases progressively to reach an asymptotic value of 20%.

To study more precisely the changes of ultimate properties with irradiation, values of stress at break (σ_R) are plotted as a function of values of ε_R for every absorbed doses (Fig. 7). For initial and some absorbed doses, tensile curves are also reported in the same figure. Usually, this rupture envelope is surimposed to the initial tensile curve [14,16]. Here, one can be observed that the plastic part of the tensile curve is shifted towards lower stress values, especially for low doses. Beyond 2000 Gy, however, an asymptotic ($\sigma_R - \varepsilon_R$) curve seems to be reached.

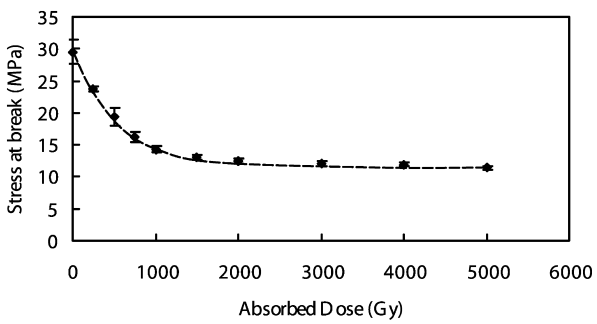

Fig. 5. Changes in stress at break vs absorbed dose.

3.3. EWF method

For the low absorbed doses (0–1500 Gy), we have shown an increase of ε_R whereas σ_R decreases (Figs. 5 and 6). What about toughness in terms of fracture mechanics approach? EWF plots of virgin and aged samples are shown in Fig. 8: w_e remains almost constant whereas βw_p undergoes significant variations and appears to be the pertinent parameter to study toughness variations as previously suggested [17,18]. Fig. 9 shows βw_p as a function of the absorbed doses: toughness increases up to an absorbed dose of 750 Gy and decreases for higher doses. Paradoxically, it appears thus that a decrease of molar mass from 6000 to 300 kg mol^{-1} leads to an increase of capacity to absorb energy and so toughness. This fact has to be linked with the observed increase of ε_R although the maximum value of ε_R and βw_p is not reached for the same absorbed dose (500 against 750 Gy for this latter). For doses upper to 1500 Gy the brittle behaviour with unstable crack propagation and confined plastic zone permits to consider βw_p equal to zero.

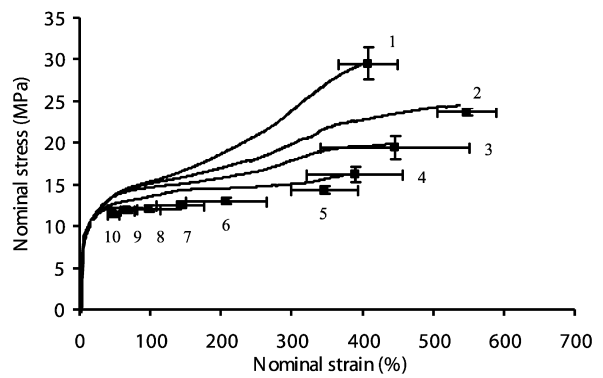

Fig. 7. Failure envelope (σ_R vs ε_R during exposure) (■) and tensile curves of initial and irradiated specimen in nominal strain stress coordinates: (1) initial, (2) 250, (3) 500, (4) 750, (5) 1000, (6) 1500, (7) 2000, (8) 3000, (9) 4000 and (10) 5000 Gy.

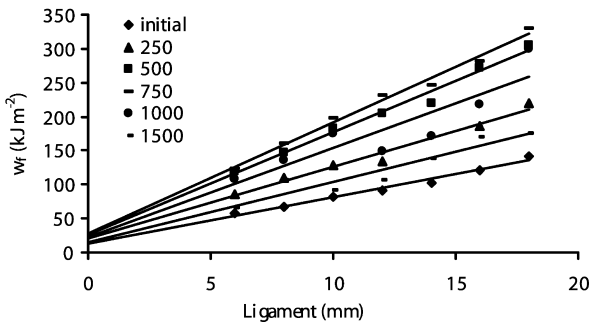

Fig. 8. Plot of specific work of fracture vs ligament length for varying absorbed dose.

3.4. Fractography

SEM photographs of the fracture surface of notched samples are shown in the case of virgin PTFE (Fig. 10) and irradiated PTFE at 1500 Gy (Fig. 11) at different magnifications. The choice of both absorbed doses is due to the fact that values of βw_p are similar although the embrittlement process has begun at 1500 Gy.

Completely different failure mechanisms are observable between both samples. Fractographies of virgin PTFE exhibit a fine fibrillar structure, with a fibril diameter of about 50 nm whereas fractographies of irradiated PTFE show broad and coarse fibrils having a diameter close to 10 μm. Theses large fibrils are composed themselves of fibrils of 50 nm. It is noticeable that such differences are induced by a variation of molar mass but do not modify toughness in term of βw_p. We can assume that, as in the case of amorphous polymers, a decrease of molar mass promotes coarser fibrils when failure by crazing mechanism occurs [19]. In other words, βw_p is determined by the extent of the outer plastic zone around the crack but not by the failure mechanism in particular by the diameter of fibrils.

3.5. Thickness profile of degradation

The above results are interpretable in terms of homogeneous degradation, only if oxidation is not diffusion controlled. An argument in favour of this hypothesis comes from the results of a parallel study showing that the PTFE lifetime was independent of the dose rate [20]. Whereas in the diffusion controlled regime, the oxidation effects would be expected to decrease when the dose rate increases.

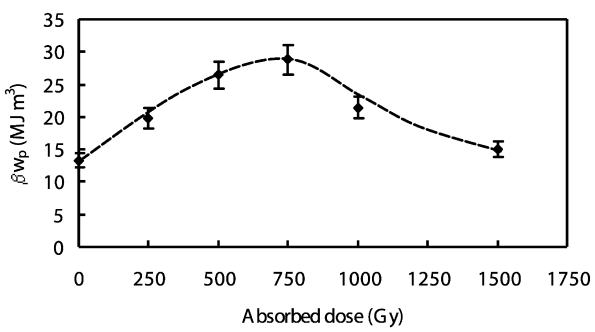

Fig. 9. Non-essential work of fracture (βw_p) as a function of absorbed dose.

4. Discussion

4.1. Molar mass changes

Irradiation leads to PTFE embrittlement and this latter is, no doubt, linked to chain scission. The number of chain scissions per mass unit $n = 1/M_n - 1/M_{n0}$ has been plotted against dose in Fig. 4. Chain scission appears to be autoaccelerated, in the early period of exposure, which is difficult to justify in the frame of a steady state radiochemical process. Indeed, a small departure from Suwa's relationship [11] could explain this curvature of the curve $n = f(D)$.

4.2. Embrittlement mechanism

The fact that the ultimate elongation ε_R varies non-monotonically with irradiation whereas molar mass decreases continuously reveals some similarity between the behaviours of irradiated PTFE and virgin high density polyethylene (hdPE). In the case of this latter, ε_R increases with the molar mass until about $5–7.5 \times 10^2$ kg mol^{-1} and then decreases slowly for very high molar mass [21,22]. This behaviour has received many qualitative explanations [23,24,25] among which one appears especially interesting in our case: In very high molar mass PE, there is a great number of non-extended intercrystalline tie chains linking the microfibrils and making the fracture difficult which results from their separation. These 'interfibrillar' ties play a crosslinking role, they tend thus to increase the strength and decrease slightly elongation.

Since non-extended tie chains are longer than extended ones, their probability to be broken by irradiation must be higher. Their 'bridging' effect on microfibrils is thus expected to disappear rapidly at the beginning of exposure. Then, what predominates is the progressive destruction of the entanglement network in the amorphous phase with a decrease of both ε_R and σ_R.

In the case of PE not of high molar mass, PP and various other polymers, it has been shown that, when they undergo a statistical chain scission ageing process, the corresponding rupture envelope $\sigma_R = f(\varepsilon_R)$ is the initial tensile curve [14,16]. In other words, ageing does not modify the tensile behaviour except in its ultimate (rupture) part. The rupture envelope of PTFE (Fig. 7) displays two distinct parts. The first one, from point 1 (unirradiated) to point 5 (1.5 kGy) corresponds to the 'bridged' PTFE. The second one (beyond point 5) would correspond to the 'non-bridged' PTFE for which the tensile curves would be surimposable. It is noteworthy that the first part of the rupture envelope corresponds well to the effect of a 'decrosslinking' for

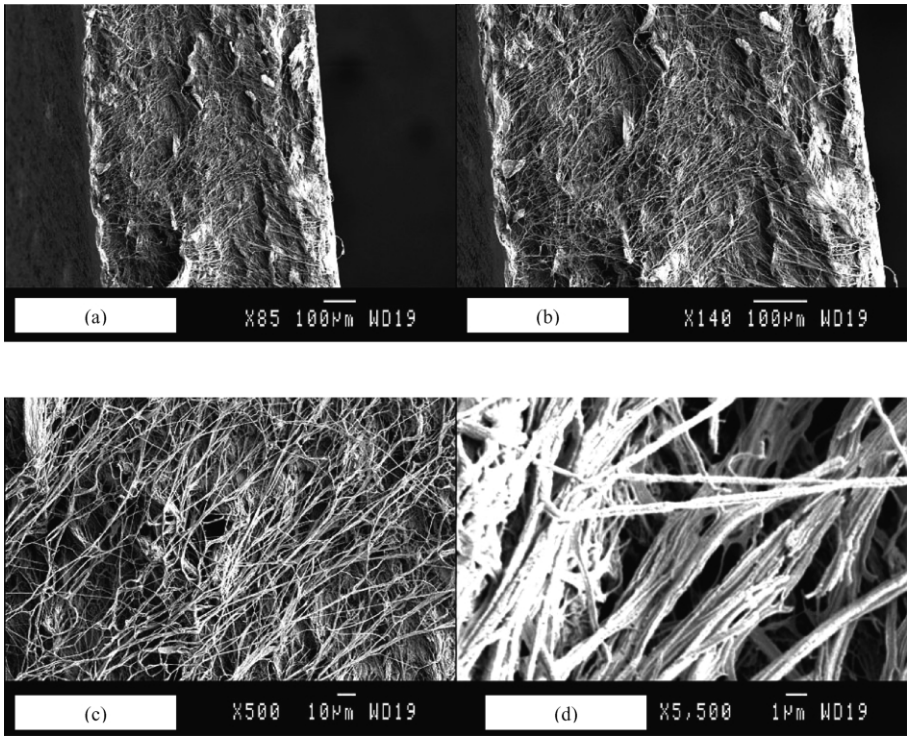

Fig. 10. SEM photographs of surface of notched non-irradiated specimen at different magnifications (a): × 85, (b): × 140, (c): × 500, (d): × 5500.

an elastomer [26]. Although the maximum of ε_R and βw_p do not coincide exactly, it can be reasonably assumed that the trends of variation, i.e. initial increase and final decrease result from the same mechanisms i.e. disappearance of interfibrillar bonding.

4.3. Embrittlement criterion and lifetime criterion

The choice of an endlife criterion is more difficult for PTFE than for polyolefins, owing to the progressive character of property variations and the absence of a well

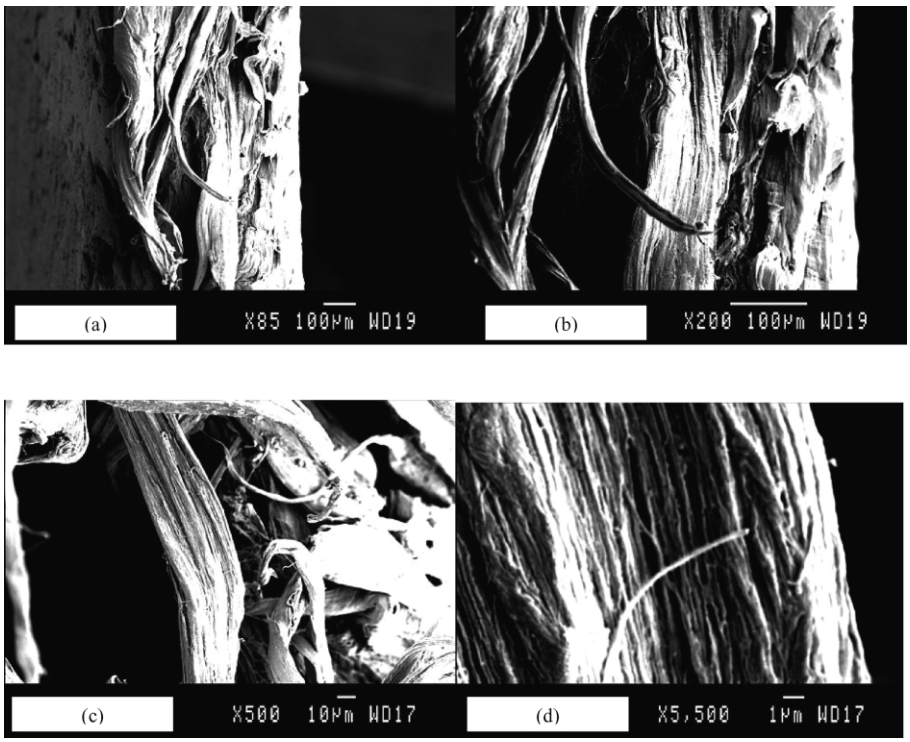

Fig. 11. SEM photographs of surface of an notched irradiated at 1500 Gy specimen at different magnifications (a): × 85, (b): × 200, (c): × 500, (d): × 5500.

marked transition between the ductile and the brittle regime as previously mentioned. This progressive character is surprising: embrittlement of semi-crystalline polymers (polypropylene [16] or polyethylene [27]) induced by chain scission process exhibits a catastrophic behaviour. However, it was shown that this catastrophic behaviour is mainly due to appearance of a necking process (or localization of plastic deformation along the calibrated zone) just after the yield [16]. For instance, the localization process explains the existence of a maximum stress in engineering tensile curve for PP or PE. In the case of PTFE, the plastic deformation is more diffuse that is why embrittlement process is more progressive.

The choice of an arbitrary criterion such as half of the initial value of ε_R or σ_R is questionable, the lifetime would be noticeably shorter for σ_R ($\sim$900 Gy) than for ε_R ($\sim$1500 Gy). The difference between both criteria (dose at half value of the strain at break or stress at break) has been already reported [28]. Furthermore, EWF method has been shown to be better to characterise the fracture behaviour of ductile polymers.

Two criteria could be used with this latter method: The first (pessimistic) one could correspond to the maximum of βw_p, i.e. to a dose of 750 Gy (Fig. 7), which coincides with the half value of σ_R and, more and less to the end of the 'bridged' fracture regime. The second (optimistic) criterion could correspond to the end of the ductile regime as assessed by EWF i.e. to a dose of $\sim$1500 Gy which is close to the dose at which the ultimate strain has been divided by two.

The advantage of the first criterion is that it corresponds to a single mechanism during which the fracture parameters as determined by EWF vary monotonically. Such characteristics are expected to simplify the kinetic modelling. The inconvenient is that, from a practical point of view, it underestimates (approximately by a factor 2) the material's lifetime. The advantages and disadvantages of the second criterion are exactly opposite. Finally, the choice of the criterion could be made in function of the application under consideration and corresponding to a given mechanical loading.

To predict lifetime, two ways can be suggested. The first and simpler one starts from the hypothesis that the degradation conversion is dose rate independent and, thus, that the lethal dose is 750 or 1500 Gy depending of the chosen option (see above).

The lifetime t_F is thus given by:

$$\int_0^{t_F} I(t)\mathrm{d}t = 750 \text{ or } 1500 \text{ Gy} \tag{6}$$

where $I(t)$ is the dose rate expressed as a function of time.

In the second, more sophisticated way, a kinetic model must be established for the number of chain scissions:

$$n = \frac{1}{M_n} - \frac{1}{M_{n0}} = f(t) \tag{7}$$

This model must describe the sigmoidal shape of the experimental curve (if this latter is well confirmed), which will probably need to use non-stationary conditions. It appears difficult, a priori, to determine if the kinetic course of chain scission is or not dose rate dependant. According to the above defined endlife criteria, the endlife molar mass could be $M_{nF} \sim 300$ kg mol^{-1} ($D_F = 750$ Gy) or $M_{nF} \sim 100$ kg mol^{-1} ($D_F = 1500$ Gy). The endlife chain scission criterion would be thus:

$$t_F = f^{-1}(n_F) \tag{8}$$

where f^{-1} is the reciprocal function of f.

4.4. Towards a generalization of the results

In the case of predominant chain scission where embrittlement results only from a molar mass decrease, it is tempting to search eventual universal features for endlife criteria because they would give a strong physical basis for lifetime prediction. In amorphous, glassy polymers, there are now numerous evidences of the sharp link between the entanglement density (the reciprocal of the molar mass M_e between entanglements) and the critical molar mass M_c' separating the ductile and the brittle regime. It may be written:

$$M_C' = qM_e \tag{9}$$

where q is the order of unity, typically between 2 and 10.

In the case of polyolefins, however, there is no clear relationship between M_c' and the entanglement density since q values of the order of 60 have been found as well for PP ($M_c' \sim 210$ kg mol^{-1} [16,29], $M_e \sim 3.5$ kg mol^{-1} [30]) as for PE ($M_c' \sim 100$ kg mol^{-1} [10,31], $M_e \sim 1.75$ kg mol^{-1} [29]).

In the case of PTFE, (as presumably for ultra high molar mass PE) the determination of the ductile–brittle critical molar mass is more difficult than for the above cited polyolefins because the transition between both regimes is more progressive. By plotting ε_R against molar mass (Fig. 12), one obtains a curve which can be considered as composed of a ductile plateau at $\varepsilon_R \sim 400\%$, a brittle plateau at $\varepsilon_R \sim 75 \pm 25\%$ and a transition spread over

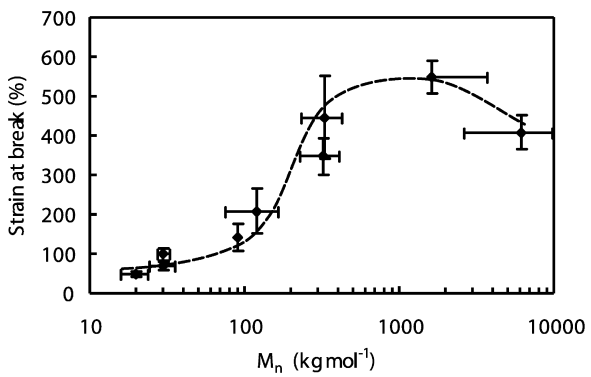

Fig. 12. Strain at break as a function of number average molar mass (M_n) for irradiated samples.

about one decade of molar masses. The inflection point has an abscissa close to $M'_c \sim 200\ \mathrm{kg\ mol^{-1}}$. Since, in PTFE, the molar mass between entanglements is $M_e = 3.7\ \mathrm{kg\ mol^{-1}}$ [32], one see that

$$q = M'_C/M_e \sim 50 \quad (10)$$

We are now able to distinguish two polymer families: the first one, for which $q < 10$, contains presumably all the amorphous polymers and many semi-crystalline polymers having a relatively low crystalline ratio or being polar (PA11, PET). As a matter a fact, for the industrial grades of these polymers, $M_{n0}/M_e < 10$ so that necessarily $q < 10$. The second family would contain the semi-crystalline polymers having relatively high crystallinity ratios or being apolar (PP, PE, PTFE): For all these polymers $q > 50$. Indeed, it will be interesting, in a next future, to determine which structural characteristic (crystallinity ratio, morphology or polarity for instance) controls the value of q and, indeed, if there are other families displaying distinct behaviours.

5. Conclusion

Molar mass and mechanical measurements were performed on PTFE samples irradiated by Co^{60} γ rays at $100\ \mathrm{Gy\ h^{-1}}$ dose rate. The molar mass decreases rapidly, it is divided by 4 after 250 Gy exposure. The change of mechanical properties reveal two successive stages. In the first one, the toughness and the ultimate elongation increase whereas the ultimate stress decreases. Beyond 500 or 750 Gy dose, depending on the testing method, all the above properties decrease and complete embrittlement is observed at 1500 Gy. This behaviour can be explained by the presence of very long chains (initial molar mass $M_n \sim 6000\ \mathrm{kg\ mol^{-1}}$) giving extended tie chains responsible for interfibrillar bridging. Their scission, in the early period of exposure, displays the characteristics of a 'decrosslinking' process in an elastomer: increase of ultimate elongation and toughness and decrease of ultimate stress.

The ductile–brittle transition corresponds to a critical molar mass M'_c of about $200\ \mathrm{kg\ mol^{-1}}$ i.e. about 50 times the molar mass between entanglements M_e in the melt. Two polymer families can be distinguished, those for which $M'_c < 10M_e$: amorphous and low crystallinity polar polymers, and those for which $M'_c \sim 50M_e$: high crystallinity and non-polar polymers.

Acknowledgements

The authors wish to acknowledge Wilfrid Seiler for X-ray experiments and Antoine Tosi for the experimental part of the work.

References

[1] Matsumae K, Watanable M. J Polym Sci 1958;28:653–63.
[2] Forsythe JS, Hill DJT. Prog Polym Sci 2000;25:101–36.
[3] Greco R, Ragosta G. Plast Rubber Process Appl 1987;7:163–71.
[4] Bersted BH, Anderson TG. J Appl Polym Sci 1990;39:499–514.
[5] Dai CA, Kramer E, Washiyama J, Hui CY. Macromolecules 1996;29:7536–43.
[6] Kudoh H, Sasuga T, Seguchi T. Polymer 1996;37:3737–9.
[7] Mai YW, Cotterell B. Int J Fract 1986;32:105–25.
[8] Wu J, Mai YW. Polym Engng Sci 1996;36:2275–88.
[9] Vu-Khan T. Theor Appl Fract Mech 1994;21:83–90.
[10] ESIS Test Protocol for Essential Work of Fracture Version 5; 1997.
[11] Suwa T, Takehisa M, Machi SJ. Appl Polym Sci 1973;17:3253–7.
[12] Separati CA, Starkweather HW. Fortschr Hochpolym-Forsch 1961;2:465–95.
[13] Kennedy MA, Peacock AJ, Mandelkern L. Macromolecules 1994;27:5297–310.
[14] Pabiot J, Verdu J. Polym Engng Sci 1981;21:32–7.
[15] Gillen KT, Celina M. Polym Degrad Stab 2001;71:15–30.
[16] Fayolle B, Audouin L, Verdu J. Polym Degrad Stab 2000;70:333–40.
[17] Haschemi S, Williams JG. Plast Rubber Compos 2000;29:294–300.
[18] Fayolle B, Audouin L, Verdu J. Polym Degrad Stab 2002;75:123–9.
[19] Sugimoto M, Ishikawa M, Hatada K. Polymer 1995;36:3675–82.
[20] Fayolle B, Audouin L. Unpublished results.
[21] Margulies AF. SPEJ 1974;27:44.
[22] Popli R, Mandelkern L. J Polym Sci Part B 1987;25:441–7.
[23] Nunes RW, Martin JB, Johnson JF. Polym Engng Sci 1982;22(4):205–27.
[24] Peacock AJ, Mandelkern L, Alamo RG, Fatou JG. J Mater Sci 1998;33:2255–68.
[25] Bayer RK, Liebentraut F, Meyer T. Colloid Polym Sci 1992;270:331–48.
[26] Gueguen V, Audouin L, Pinel B, Verdu J. Polym Degrad Stab 1994;46:113–22.
[27] Lassiaz M, Pouyet J, Verdu J. J Mater Sci 1994;29:2177–81.
[28] Abdou SM, Mohamed RI. J Phys Chem Solids 2002;63:393–8.
[29] Fayolle B, Audouin L, Verdu J. Submitted for publication J. Polym Sci Part B.
[30] Van Krevelen DW. Properties of Polymers, Third ed. Amsterdam: Elsevier; 1990. p. 465.
[31] Jordens K, Wilkes GL, Janzen J, Rohlfing DC, Welch MB. Polymer 2000;41:7175–92.
[32] Mark JE, editor. Physical Properties of Polymer Handbook. Woodburg, New York: American Institute of Physics Press; 1996. p. 339.